Journal Pre-proof

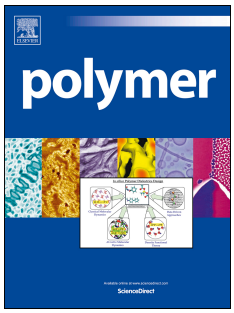

On the mechanical properties of melt-blended nylon 6/ethylene-octene copolymer/ graphene nanoplatelet nanocomposites

Suhail Attar, Biqiong Chen, Gianluca Cicala, Giuseppe Catalanotti, Tommasso Scalici, Brian G. Falzon

PII: S0032-3861(22)00106-9

DOI: https://doi.org/10.1016/j.polymer.2022.124619

Reference: JPOL 124619

To appear in: *Polymer*

Received Date: 19 November 2021

Revised Date: 29 January 2022

Accepted Date: 2 February 2022

Please cite this article as: Attar S, Chen B, Cicala G, Catalanotti G, Scalici T, Falzon BG, On the mechanical properties of melt-blended nylon 6/ethylene-octene copolymer/graphene nanoplatelet nanocomposites, *Polymer* (2022), doi: https://doi.org/10.1016/j.polymer.2022.124619.

Author's contribution statement

Suhail Attar: Conceptualization, Methodology, Investigation, Formal analysis, Writing - Original Draft

Biqiong Chen: Supervision, Conceptualization, Methodology, Reviewing and Editing

Gianluca Cicala: Resources

Giuseppe Catalanotti: Supervision, Resources, Project administration

Tommasso Scalici: Resources, Project administration

Brian Falzon: Supervision, Conceptualization, Resources, Reviewing and Editing, Project administration, Funding acquisition

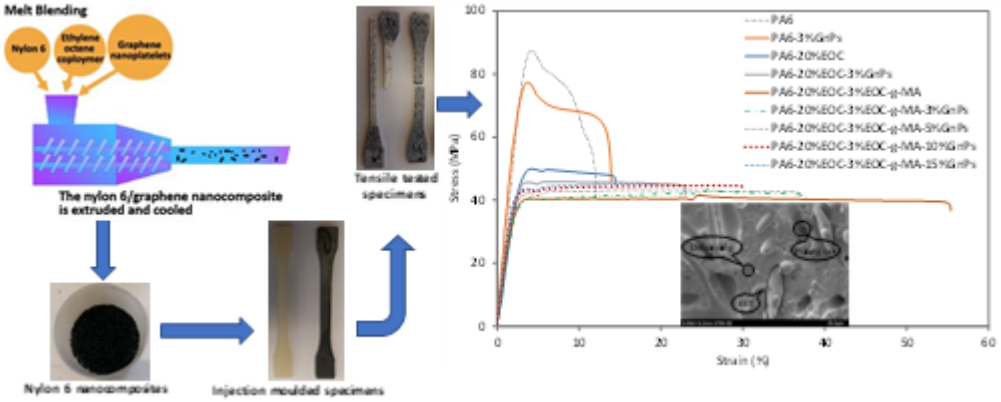

On the mechanical properties of melt-blended nylon 6/ethylene-octene copolymer/graphene nanoplatelet nanocomposites

Suhail Attar[a], Biqiong Chen[b], Gianluca Cicala[c], Giuseppe Catalanotti[d], Tommasso Scalici[e], Brian G. Falzon[f]

[a,b,d,e] School of Mechanical and Aerospace Engineering, Queen's University Belfast, Ashby Building, Stranmillis Road, Belfast BT9 5AH, United Kingdom.

[c] Department of Civil Engineering and Architecture, University of Catania, Edificio 10 V.le A.Doria, 6 - 95125 Catania, Italy

[f] School of Engineering, STEM College, RMIT University, GPO Box 2476, Melbourne 3001, Victoria, Australia

Abstract

Ethylene-octene copolymer (EOC) with a loading level of 20 wt%, maleated EOC (EOC-g-MA) with a loading level of 3 wt% and graphene nanoplatelets (GnPs) at four different loading levels, i.e., 3 wt%, 5 wt%, 10 wt% and 15 wt% were added to nylon 6 to prepare nanocomposites using a twin-screw extruder with a high shear rate screw running at 300 rpm. Increased stiffness was observed with the addition of GnPs while tensile strength of nanocomposites was only slightly influenced. Addition of GnPs into nylon 6 and nylon 6/EOC blend caused either a reduction in the Charpy impact strength or it remained unaffected. Similarly, the Izod impact strength of compatibilized nylon 6/EOC blend increased while that of nylon 6/EOC blend-based nanocomposites decreased. An increase was observed in the compressive Izod impact strength of compatibilized nylon 6/EOC blend. Addition of GnPs to nylon 6/EOC blend caused an increase in the fracture toughness due to their influence on the morphology and fracture mechanisms. This study shows that simultaneous addition of high surface area GnPs and an impact modifier to neat nylon 6 can help achieve enhancement and tailoring of stiffness and toughness.

Keywords

Nylon 6, graphene, elastomer, nanocomposites, mechanical properties.

1. Introduction

Development of polymer nanocomposites that possess a unique balance of properties is an area of great interest. Simultaneous addition of stiff and elastomeric particles to the host polymer may provide simultaneous improvement of the stiffness and toughness. However, the morphology of nanocomposites also dictates the mechanical properties [1–4]. Three different types of morphologies usually obtained in the case of polymer blend-based nanocomposites are (i) encapsulated, (ii) core-shell and (iii) dispersed phase [5]. In the case of encapsulated morphology, the nanoparticles reside in the elastomeric phase which lowers the toughening capability of the dispersed elastomeric phase while in the case of core-shell morphology, nanoparticles surround the elastomeric dispersed phase in the form of a shell which proves favourable for toughness enhancement. In the case of dispersed phase morphology, most of the nanoparticles reside in the host polymer matrix and stiffness is enhanced while toughness is adversely affected.

Different research efforts have been carried out to investigate the toughening of nylon 6 using different types of rubbers and nanoparticles [6-8]. The influence of addition of clays to nylon 6/elastomer blends with different elastomers like ethene-propene rubber (EPR), natural rubber (NR)/epoxidized natural rubber (ENR), styrene-ethylene-butylene-styrene (SEBS), ethylene-octene copolymer (EOC) and carboxylated styrene-butadiene rubber (CSBR) [1], [9-10] have been investigated. Addition of different elastomers caused an enhancement of elongation at break and toughness, particularly in the case of maleated elastomers. Stiffness and strength of the blend were however adversely affected

by the addition of elastomers. Clays caused an enhancement of the stiffness with an embrittlement effect, alongside a reduction in the strength. Simultaneous addition of the elastomers and clays helped achieve balanced properties.

Single layer graphene is estimated to have a Young's modulus of 1 TPa and a tensile strength of about 130 GPa [11]. These exceptional mechanical properties of graphene have made it a potential reinforcing filler. Thanh et al. [12] studied the influence of addition of GnPs and EPR, an ethene-methacrylate copolymer (EMA), and an aminated polybutadiene (ATB) elastomer, on the structure and properties of nylon 6 nanocomposites. The addition of both GnPs and elastomers caused an enhancement of stiffness and stress at break. Toughness of all blend-based nanocomposites was however observed to decrease by the addition and increased content of GnPs. A study was carried out by Hoor et al. [13] to investigate the effect of addition of graphene nanosheets on the properties of SEBS elastomer toughened nylon 6. Addition of maleic anhydride up to 6 wt% decreased the modulus and tensile strength of nylon 6/SEBS blend while impact strength and elongation at break were increased. Kelnar et al. [14] carried out further investigation to study the effect of graphene oxide on the structure and properties of EPR rubber based impact modified PA 6. Combination of EPR and GO yielded a polyamide material with increased strength, stiffness, and toughness.

Some investigations have been directed to study the toughening effect of EOC. Norhayani et al. [15] studied the effect of addition of EOC and EOC-g-MA on the impact and tensile properties of polyamide 6 nanocomposites. Lim et al. [16] investigated the impact fracture behaviour of nylon 6/EOC-g-MA/clay-based ternary nanocomposites. A similar investigation using maleated EOC and organoclay was conducted by Chiu [9] with nylon 6 as the matrix. Addition of maleated EOC proved to be beneficial for the enhancement

of toughness and impact strength. Morphology of the blend was also influenced by the addition of compatibilizer which caused a smaller sized dispersed phase. Addition of clay was however detrimental to the toughness and strength as observed in other investigations using different elastomers.

Based on the literature study, it is identified that an investigation on the effect of addition of EOC and high surface area GnPs to nylon 6 would be a significant supplement to the available literature. GnPs with high surface area could possibly generate large volume of interfacial area and substantially influence the tensile and impact properties. Nylon 6/EOC/GnPs nanocomposites are therefore prepared in this study to investigate the effect of simultaneous addition of these additives on the mechanical properties.

2. Experimental

2.1. Materials

Nylon 6 (Akulon® F223-D from DSM Engineering Plastics) and ethylene-octene copolymer (Engage 8150 from DuPont Dow Elastomers) were purchased from ResinEx UK. Graphene nanoparticles with a surface area of 500 m^2/g were supplied by ThermoFisher Scientific. Maleated EOC (EOC-g-MA, Fusabond 463) was provided by DuPont Dow Elastomers.

2.2. Preparation of nylon 6 nanocomposites

Nylon 6 pellets were cryogenically ground using a Wedco SE-12 UR pilot plant grinding mill at 7000 rpm and a gap size 400 µm. The powder size distribution was found to be 100-300 µm using a stereo microscope (Nikon SMZ800). Nylon 6 powder was dried overnight at 80 ^oC using a dryer (Carbolite). Pre-mixing of nylon 6 with 3, 5, 10 and 15

wt% of GnPs and 3 wt % EOC-g-MA was done using a Thermo Scientific Prism Pilot 3 High Speed Mixer at 3000 rpm for 4 minutes. Melt blending of nanocomposites was performed on a Thermo fisher twin-screw extruder (HAAKE) using a high shear screw design at 300 rpm and two melt blending cycles. During the first cycle, nylon 6, EOC-g-MA and GnPs were melt blended and the extrudate was pelletized. In the second cycle, the extruded pellets were melt blended with EOC pellets to give final nanocomposite materials. The temperature of the extruder barrel was 260 ^{o}C for zone 1-3, 270 ^{o}C for zone 4-5 and 260 ^{o}C for the die.

2.3. Characterisation of nylon 6 nanocomposites

Fourier Transform Infrared Spectroscopy (FTIR) was carried out using a Perkin Elmer Spectrum 100 spectrometer with an ATR sampling accessory. All the spectra were recorded at a resolution of 4 cm^{-1} with 32 scans in mid infrared region of 4000-650 cm^{-1}. Differential scanning calorimetry (DSC) was carried out using Perkin Elmer DSC model 6 under an inert nitrogen environment. A heating rate of 10 ^{o}C/min was used to heat the samples between 30 ^{o}C and 250 ^{o}C, held at 250 ^{o}C for 2 mins, then cooled to 30 ^{o}C at 10 ^{o}C/min and reheated to 250 ^{o}C at 10 ^{o}C/min. A second heating curve was used for the calculation of degree of crystallinity.

Tensile tests were conducted according to BS ISO 527 at room temperature using a Zwick testing machine with a 10 kN load cell and a crosshead speed of 5 mm/min. Five specimens were tested for each material. Dog-bone tensile test specimens were prepared by injection moulding using a Rondol high force 5 small injection moulding machine according to BS ISO 527 (Type 1BA) standard.

Charpy impact tests were conducted at room temperature using a Resil impact tester with a 7.5 J hammer according to BS ISO 179. A total of ten specimens were tested. Izod impact tests were conducted in tension (notch opening) mode and compression (notch closing) mode, again using a Resil impact tester with a 7.5 J hammer. A total of eight specimens were tested. Charpy impact, Izod impact and Single edge notch three-point bend test (SENB-3PB) specimens were prepared using a tabletop injection moulding machine (MegaTech H7/18, TecnicaDueBi, Fabriano, Italy) as per BS ISO 179 standard. The temperature of the feed zone was 20 ^{o}C, 200 ^{o}C for zone 1, 240 ^{o}C for zone 2, 260 ^{o}C for the injection cylinder and 20 ^{o}C for the mould.

SENB-3PB tests were conducted using a Zwick Z100 testing machine at a loading speed of 5 mm/min and a 10 kN load cell. SENB-3PB specimens were prepared by introducing cracks of length 2.25, 3, 3.75, 4.5, 5.25 and 6 mm, with a handheld blade, in the injection moulded rectangular bars (80 x 10 x 4 mm). Load displacement curves of the test specimens were recorded and the work done to the point of crack propagation (maximum load point on the curve) was used for J integral calculations.

Scanning Electron Microscopy (SEM) was conducted using a FlexSEM 1000 scanning electron microscope at 5 kV. Samples were prepared by cutting small segments from representative Charpy impact tested and 3-point SENB tested specimens. Gold coating of the stub-mounted specimens was performed using an Agar Scientific sputter with a current of 30 mA and vacuum of 0.05 mB, for 240 sec.

3. Results and discussion

3.1. Structure

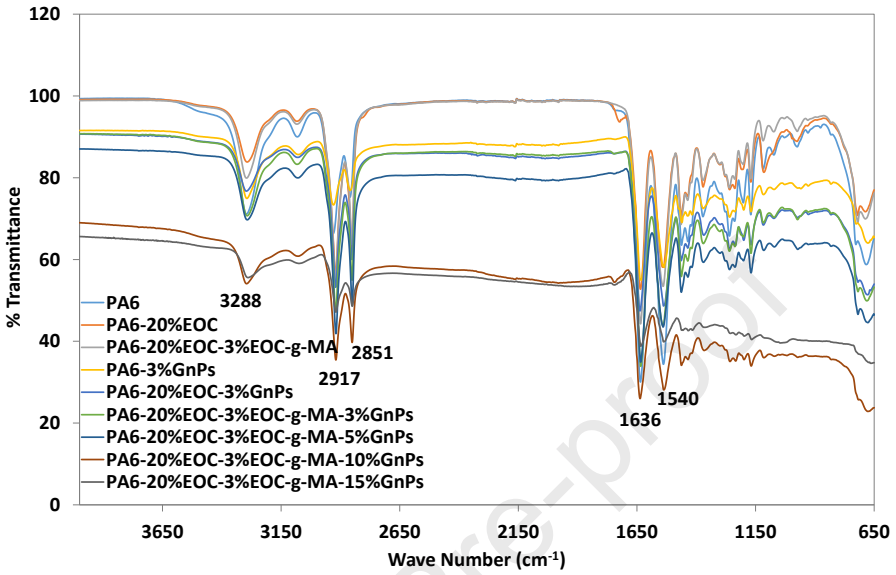

Figure 1 FITR spectra of nylon 6, nylon 6/EOC blends and nylon 6/EOC/GnPs nanocomposites

FTIR scans of samples, shown in Figure 1, were performed to see any possible interactions between different constituents. Strong bands observed at 3288 cm^{-1}, 2917 cm^{-1} and 2851 cm^{-1} for nylon 6 represent N-H stretching vibration of the amide linkage and asymmetric and symmetric stretching vibrations of aliphatic C-H bonds respectively [17]. Two other strong IR bands are observed at 1636 cm^{-1} and 1540 cm^{-1} corresponding to the C=O stretching vibration of the amide-I and N-H bending vibrations of the amide-II respectively [4]. GnPs were expected to have a weak interaction with nylon 6, EOC or EOC-g-MA due to the absence of any functional groups and no new absorption peaks were observed in case of nanocomposites as compared to that of the neat nylon 6 spectrum. FTIR scans of nylon 6/ EPR/ EMA/ATB/GnPs nanocomposites by Thanh et al. [12] also showed a similar spectrum to the one observed here. No interfacial

interaction was observed between nylon 6 and EOC, possibly due to immiscibility of the two polymers.

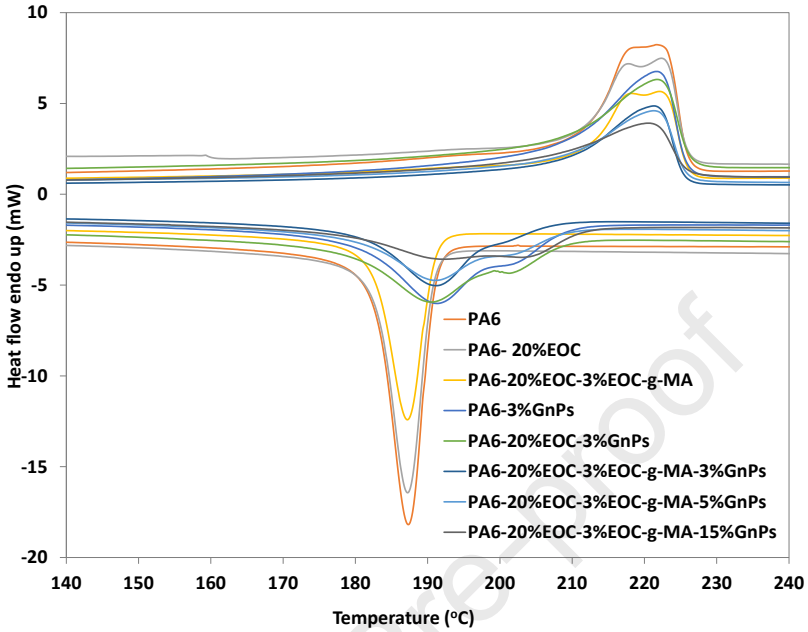

Figure 2 Cooling and 2nd DSC heating curves for nylon 6 and nylon 6 nanocomposites

Table 1 DSC results for nylon 6, nylon 6/EOC and nylon 6/EOC/GnPs nanocomposites

Sample ID	2nd Heating			Cooling
	Melting Temp T_m (°C)	Enthalpy of fusion ΔH (J/g)	% Crytallinity X_c (%)	Crystallization Temp T_c (°C)
PA6	220.1	70.5	37.5	189.0
PA6-20%EOC	220.8	57.5	38.2	188.8
PA6-20%EOC-3%EOC-g-MA	220.7	46.8	32.3	188.7
PA6-3%GnPs	220.2	64.1	35.1	192.8
PA6-20%EOC-3%GnPs	220.2	58.8	40.6	191.9
PA6-20%EOC-3%EOC-g-MA-3%GnPs	219.9	53.9	38.7	192.5
PA6-20%EOC-3%EOC-g-MA-5%GnPs	219.9	49.8	36.8	192.5
PA6-20%EOC-3%EOC-g-MA-15%GnPs	219.2	42.6	36.5	193.3

DSC scans of samples were performed to investigate any influence of the addition of EOC and GnPs on the melting and crystallization behaviour of nylon 6. Second heating and cooling DSC curves of nylon 6 and nanocomposites are shown in Figure 2. Measured parameters for all the samples are tabulated in Table 1.

The second heating curve of neat nylon 6 showed two peaks, a lower one at 214 ^{o}C for γ-crystallites and a higher peak at 220 ^{o}C for α-form crystals [18] Addition of EOC to neat nylon 6 had little or no effect on the α or γ crystalline phases of neat nylon 6 and two melting peaks were observed at 214 ^{o}C and 216 ^{o}C [19]. Addition of the compatibilizer EOC-g-MA to the nylon 6/EOC blend again showed a heating curve with two melting peaks at 214 ^{o}C and 220 ^{o}C. Graphene nanoparticles were added to neat nylon 6, nylon 6/EOC blend and compatibilized nylon 6/EOC blend. Low temperature melting peak disappeared with the addition of GnPs due to the possible stabilizing effect of GnPs favouring the creation of more stable α-crystallites. A degree of crystallinity of 35.1% was observed for nylon 6/GnPs nanocomposites. Addition of GnPs to nylon 6 caused a mild reduction in the crystallinity while the addition of EOC to nylon 6 had no effect on the crystallinity of neat nylon 6.

Addition of 3 wt% GnPs to nylon 6/EOC blend had a minor influence on the degree of crystallinity while the melting temperature remained unaffected. A crystallinity of 40.6% for blend-based nanocomposites was slightly higher than that for the corresponding nylon 6/EOC blend. A crystallinity of 38.7% was observed for nylon 6/EOC/EOC-g-MA/GnPs nanocomposites which was higher than the crystallinity of corresponding compatibilized nylon 6/EOC blend. Different higher contents of GnPs like 5 wt%, 10 wt% and 15 wt% were added to the compatibilized nylon 6/EOC blend. The crystallinity had values of 38.7% for 3 wt% GnPs nanocomposites and 36.5% for 15 wt% GnPs nanocomposites. A much higher crystallinity of 60.7% was observed for 10 wt% GnPs based nanocomposites, which could be due to the fact that the nucleating effect of GnPs might have overcome the hindering effect. GnPs can simultaneously act as nucleating sites for the formation of crystals while they may also hinder the formation of crystals. These two

influences depend on different factors including the size, loading level and interaction of GnPs with the host polymer and one influence may overcome the other based on these factors.

3.2. Mechanical properties

Tensile tests of neat nylon 6 and nanocomposite samples were carried out to measure the tensile properties and representative curves are shown in Figure 3. Strain varied linearly with applied stress for all samples up to the elastic limit and became non-linear beyond this. Stress-strain curves of nanocomposites with different wt% of GnPs showed a reduction in the elongation at break with increasing GnPs content as indicated by their respective stress-strain curves. Breaking strength of nanocomposites with different wt% of GnPs was close to that of the ultimate tensile strength and a plateau is observed in most of the stress-strain curves. Measured values of tensile properties are tabulated in Table 2.

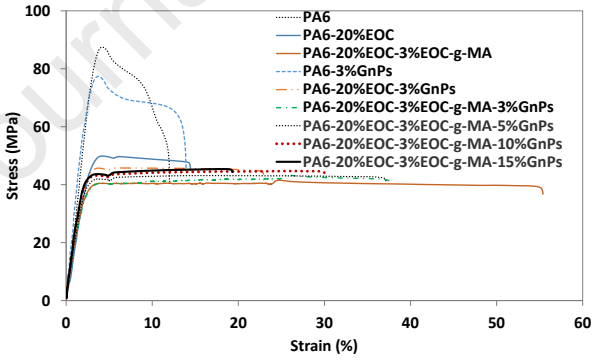

Figure 3 Representative tensile stress-strain curves for nylon 6, and nylon 6 nanocomposites

Table 2 Tensile test results of nylon 6 and nylon 6 nanocomposites

Materials	Young's modulus (GPa)	Tensile strength (MPa)	Strain at break (%)	Toughness (J/m^3)
PA6	2.8±0.2	87.0±0.5	11.8±0.6	806.9±34.8
PA6+20%EOC	1.8±0.1	50.3±0.5	14.8±0.4	678.5±25.0
PA6+20%EOC+ 3%EOC-g-MA	1.5±0.1	40.2±0.2	54.6±1.8	2160.7±72.8
PA6+ 3%GnPs	3.3±0.1	77.4±0.4	15.0±0.5	979.6±31.9
PA6+20%EOC+ 3%GnPs	1.9±0.0	45.8±0.3	22.4±0.5	977.6±27.8
PA6+20%EOC+ 3%EOC-g-MA+3%GnPs	1.6±0.0	42.2±0.7	36.8±1.0	1487.3±39.2
PA6+20%EOC+ 3%EOC-g-MA+5%GnPs	1.8±0.0	42.6±0.4	34.6±1.1	1461.8±47.6
PA6+20%EOC+ 3%EOC-g-MA+10%GnPs	2.0±0.0	43.2±0.4	29.2±1.0	1264.2±54.5
PA6+20%EOC+ 3%EOC-g-MA+15%GnPs	2.2±0.1	44.7±0.8	19.4±0.4	837.0±23.7

Nylon 6 showed a stiffness of 2.8±0.2 GPa while the highest stiffness value of 3.3±0.1 GPa (18.1% higher) was observed for 3 wt% GnPs nanocomposites. Constrained polymer chains and high stiffness of GnPs have likely increased the stiffness of nylon 6/GnPs nanocomposites [20–22]. Neat nylon 6 exhibited the highest tensile strength of 87.0±0.5 MPa and nylon 6/GnPs nanocomposites had a lower value of 77.4±0.4 MPa. A weak interface between the two constituents have likely caused this reduction in the tensile strength. However, strain at break for neat nylon 6 was increased from 11.8±0.6% to a value of 15.0±0.5% for nylon 6/GnPs nanocomposites and toughness also increased by 21.3%. An increase in the strain at break of nylon 6/GnPs nanocomposites was likely facilitated by the large surface area GnPs promoting the slippage of polymer chains. The increase in toughness could be a possible outcome of the tortuous crack propagation path caused by high surface area GnPs.

Addition of EOC to nylon 6 caused a reduction in the Young's modulus and tensile strength while elongation at break was increased. Young's modulus of nylon 6/EOC blend and nylon 6/EOC/GnPs nanocomposites was 1.8±0.1 GPa and 1.9±0.0 GPa respectively. Nylon 6/EOC/GnPs blend based nanocomposites showed a low tensile strength of 45.8±0.3 MPa and an elongation at break of 22.4±0.5%. Addition of GnPs to compatibilized nylon 6/EOC blend resulted in an increased elongation at break. Young's modulus of the nylon 6/EOC/EOC-g-MA/GnPs nanocomposites increased from 1.6±0.0 GPa for 3 wt% GnPs based nanocomposites to 2.2±0.1 GPa for 15 wt% GnPs based nanocomposites. Tensile strength of these samples varied only in the range of 42.2±0.7 MPa to 44.7±0.8 MPa, all close to the tensile strength values of the corresponding compatibilized blend. A nearly constant tensile strength upon increasing the GnPs content indicates that tensile strength is not significantly influenced by the loading level of GnPs.

Addition of higher wt% of GnPs to nylon 6/EOC/EOC-g-MA nanocomposites lowered the strain at break due to the embrittlement effect of GnPs and constraining of higher volume of polymer chains. Highest elongation at break of 54.6% and corresponding highest toughness of 2160 J/m^3 was observed for compatibilized nylon 6/EOC blend.

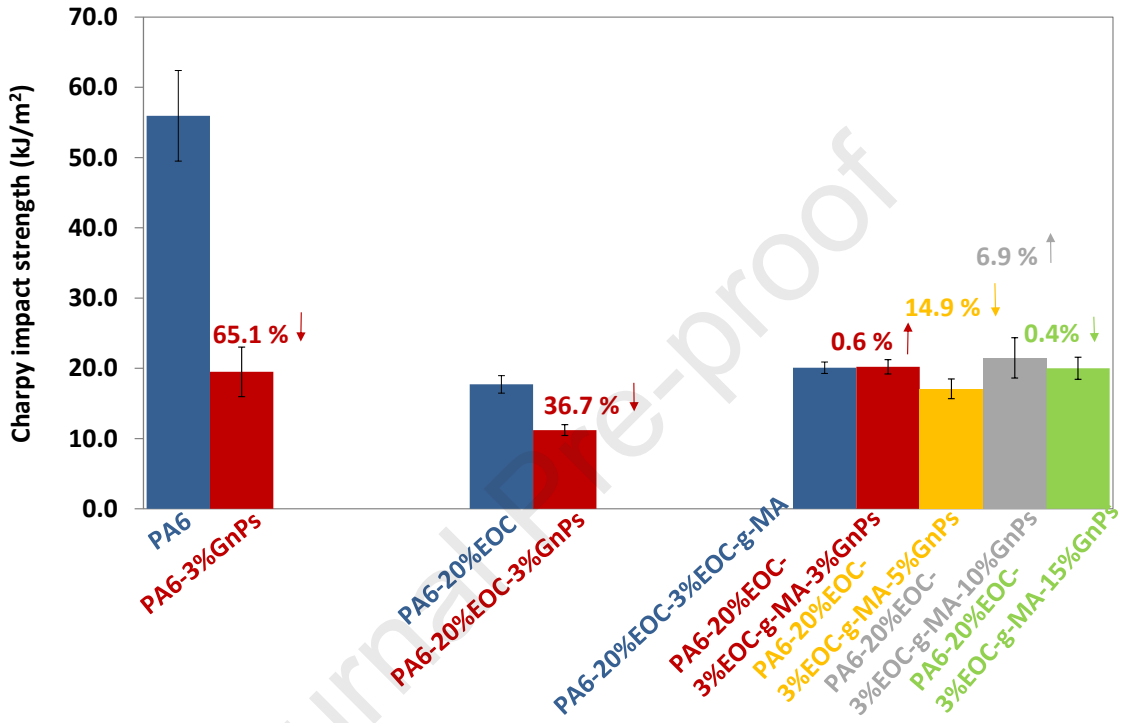

Figure 4 Charpy Impact strength of nylon 6 and nylon 6/GnPs nanocomposite samples

Measured Charpy impact strength values of nylon 6 and nylon 6 based nanocomposites are shown in Figure 4. Neat nylon 6 had the highest impact strength of 55.9±6.5 kJ/m^2 while nanocomposites with 3 wt% GnPs had a value of 19.5±3.5 kJ/m^2. This reduction in the impact strength can be attributed to the constraining of polymer chains and presence of stiff nanoparticles. Addition of EOC to neat nylon 6 caused a reduction in the impact strength of the nylon 6 while addition of EOC-g-MA to nylon 6/EOC blend caused a slight increase in its impact strength. Reduction in the impact strength of nylon 6/EOC

blend could be due to a weak interaction between the two constituents because of their immiscibility.

Nylon 6/EOC blend-based nanocomposites exhibited an impact strength value of 11.2±0.8 kJ/m^2. Addition of 3 wt% GnPs to the compatibilized nylon 6/EOC blend caused no appreciable influence on the impact strength of the compatibilized blend. The addition of higher contents of GnPs only slightly influenced the impact strength of the compatibilized nylon 6/EOC blend. Impact strength of 5 wt%, 10 wt% and 15 wt% GnPs blend-based nanocomposites was 17.0±1.4 kJ/m^2, 21.5±2.9 kJ/m^2 and 20.0±1.6 kJ/m^2 respectively. Increase in the impact strength after the addition of GnPs to compatibilized nylon 6/EOC blend, could be due to enhanced interaction between nylon 6 and EOC facilitated by maleic anhydride groups.

Izod impact strength (tension and compression mode) were also measured for the nanocomposites and detailed results are provided in the supplementary information. Fracture toughness of nylon 6 and nylon 6 blend based nanocomposites was determined by using the J-integral approach [23–25]. The area under the load displacement curve of the SENB test was used to calculate the J-integral fracture toughness [23] (details provided in the supplementary information) and plotted as a bar chart as shown in Figure 5.

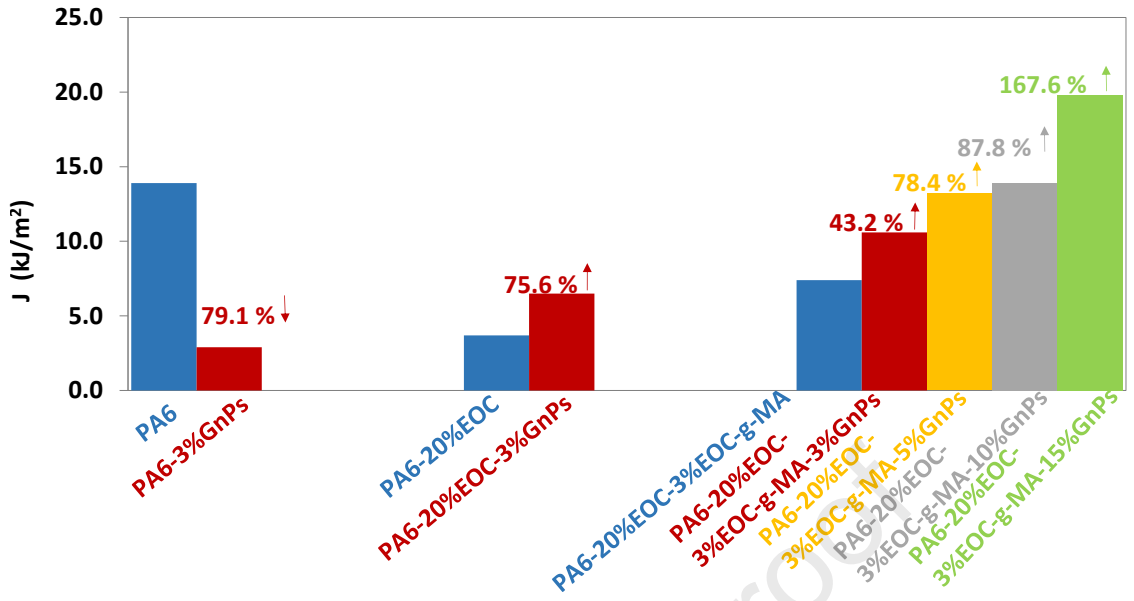

Figure 5 J-integral fracture toughness for nylon 6 and nylon 6/EOC/GnPs nanocomposites

Neat nylon 6 exhibited a critical J-integral fracture toughness of 13.9 kJ/m^2 while nylon 6/GnPs nanocomposites possessed a much lower fracture toughness. Nylon 6/EOC blend exhibited a fracture toughness of 3.7 kJ/m^2 and its nanocomposites showed a higher fracture toughness of 6.5 kJ/m^2.

Compatibilized nylon 6/EOC blend exhibited a fracture toughness of 7.4 kJ/m^2 while its nanocomposites having 3 wt% GnPs showed a higher fracture toughness of 10.6 kJ/m^2. Similarly, nanocomposites with 5 wt%, 10 wt% and 15 wt% GnPs had a fracture toughness of 13.2 kJ/m^2, 13.9 kJ/m^2 and 19.8 kJ/m^2 respectively. A trend of gradual increase in the fracture toughness was observed by increasing the content of GnPs in blend-based nanocomposites.

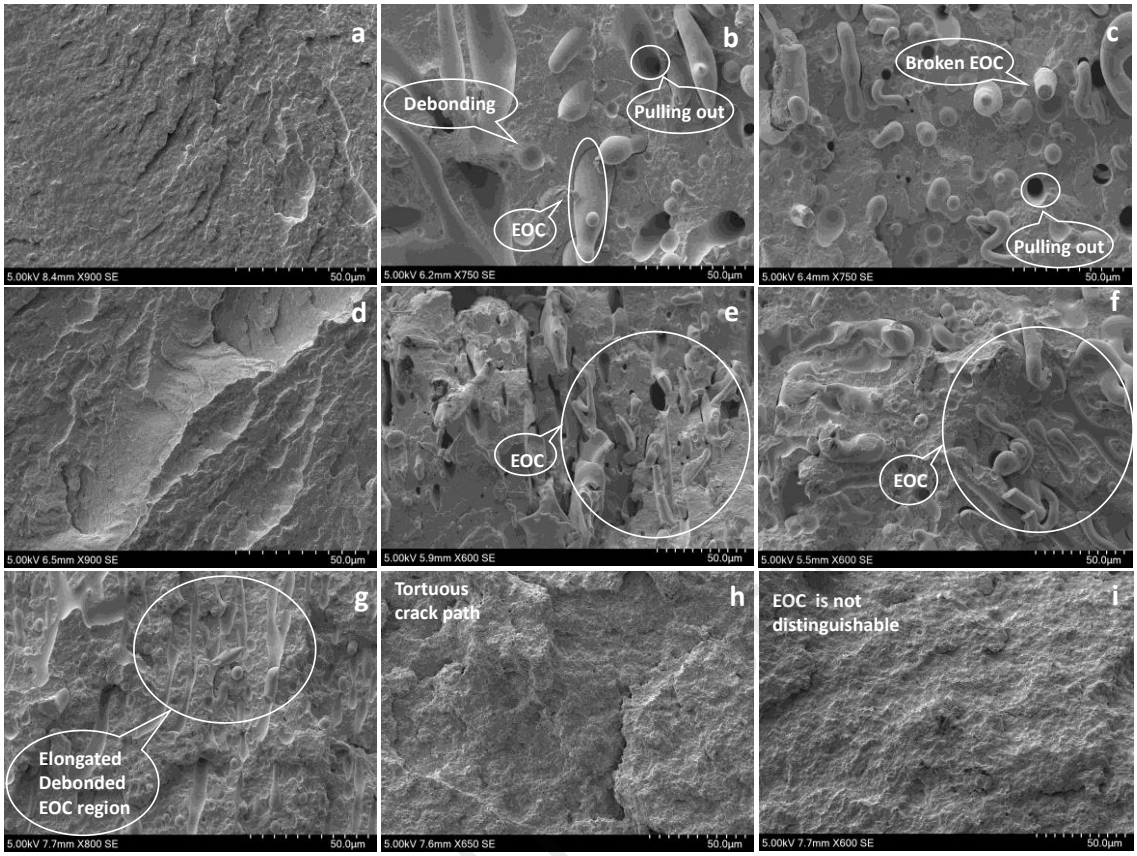

Figure 6 SEM images of the fracture surface of Charpy impact tested specimens: (a) nylon 6, (b) nylon 6/EOC, (c) nylon 6/EOC/EOC-g-MA (d) nylon 6/GnPs, (e) nylon 6/EOC/3% GnPs, (f) nylon 6/EOC/EOC-g-MA/3% GnPs(g) nylon 6/EOC/EOC-g-MA/5% GnPs(h) nylon 6/EOC/EOC-g-MA/10% GnPs and (i) nylon 6/EOC/EOC-g-MA/15% GnPs

Fracture surface morphology of Charpy impact tested samples was studied by SEM scans shown in Figure 6 (a-i). Figure 6 (a) shows the 'seashore' like fracture surface morphology of neat nylon 6. The fracture surface of nylon 6/EOC blend in Figure 6 (b) indicates the presence of dispersed EOC phase domain in the nylon 6 matrix. Several EOC particles have debonded from the nylon 6 matrix and some EOC particles have been pulled out. Debonding of EOC particles from nylon 6 matrix indicates a weak interface between nylon 6 and EOC. A significant reduction in the impact strength of nylon 6/EOC blend as compared to neat nylon 6 can be attributed to their weak interfacial interaction.

Compatibilized nylon 6/EOC blend in Figure 6 (c) shows that smaller EOC particles are present in the nylon 6 matrix compared to the previous case. Also, some fractured or

elongated EOC particles can be observed on the fracture surface which indicates that the EOC particles were pulled apart during the fracture process. It can be postulated that a stronger interface existed in this case as compared to that of uncompatibilized blend that caused more energy dissipation and an improvement in the impact strength. Nylon 6/GnPs nanocomposite sample shown in Figure 6 (d) exhibits 'sea waves' like surface morphology. Little or no agglomerates of GnPs were observed, which indicated relatively good dispersion of nanoparticles. Nylon 6/EOC/3 wt% GnPs nanocomposites shown in Figure 6 (e) exhibited slightly different morphology than that of nylon 6/EOC blend shown in Figure 6 (b). An uneven fracture surface indicates a tortuous crack propagation path possibly due to the addition of GnPs. Debonding and pulling out of EOC particles along with porosity was also observed on the fracture surface in this case. The morphology of nylon 6/EOC/EOC-g-MA/GnPs nanocomposites as shown in Figure 6 (f) was similar to that of the compatibilized nylon 6/EOC blend. However, EOC particles in compatibilized nylon 6/EOC nanocomposites were observed to be smaller than those in the case of the corresponding blend, which might have caused an improvement in the impact strength.

Compatibilized nylon 6/EOC/GnPs nanocomposites with 5 wt% GnPs showed a slightly different morphology as shown in Figure 6 (g). EOC particles became elongated in this case and debonded from nylon 6 upon application of the impact load. A minor reduction in the impact strength in this case could also be due to low energy dissipation during the debonding of EOC particles. A considerable difference in the phase morphology was observed in case of 10 wt% GnPs nanocomposites as shown in Figure 6 (h). It was difficult to distinctively observe the EOC particles in this case due to a significant reduction in the size of the dispersed phase domain. Similarly, nanocomposites with 15

wt% GnPs shown in Figure 6 (i) exhibited a morphology where the EOC phase was not distinguishable indicating possibly the formation of a co-continuous morphology.

Crack initiation and propagation phenomenon was studied by taking SEM images of SENB tested samples at three different locations i.e. at the front, middle and end of the crack surface. A nearly plain fracture surface for neat nylon 6 was observed as shown in Figure 7 (1(a-c)). Stretching of nylon 6 matrix was observed to have increased from the crack front till the crack termination. Nylon 6/EOC blend showed a rough surface morphology as shown in Figure 7 (2 (a-c)). Fibrillation of nylon 6 and drawing/pulling out of EOC particles was observed from crack initiation through to crack termination. Stretching of compatibilized nylon 6/EOC blend was also observed with little to no stretching and pulling out of EOC particles. Distinct EOC particles were hardly observed in this case which was possibly due to the compatibilization and reduction of interfacial tension among EOC and nylon 6. Addition of GnPs to nylon 6 caused constraining of the polymer chains and very little stretching or deformation was observed on the fractured surface. Nylon 6/3 wt% GnPs based nanocomposites shown in Figure 7 (4 (a-c)) exhibited a rough surface morphology with small plastic deformation or stretching across the whole facture surface. Nylon 6/EOC blend-based nanocomposites showed a combination of stretching of nylon 6 and pulling out of EOC as shown in Figure 7 (5 (a-c)). Very little pulling out and more stretching of the nylon 6/EOC bled was observed for compatibilized nylon 6/EOC blend-based nanocomposites as shown in 7 (5 (a-c)). Increasing GnPs contents to 5 and 10 wt% caused more fibrillation, however, the fibril size progressively became smaller. Stretching and fibrillation of nylon 6 and EOC was observed over the whole surface of SENB tested samples as shown in Figure 7 (2,3,5-8). In all cases, no significant difference was observed in the fracture surface morphology from the crack

front towards the crack end. It is assumed that quasi-static loading conditions caused a stable crack propagation through the SENB specimens.

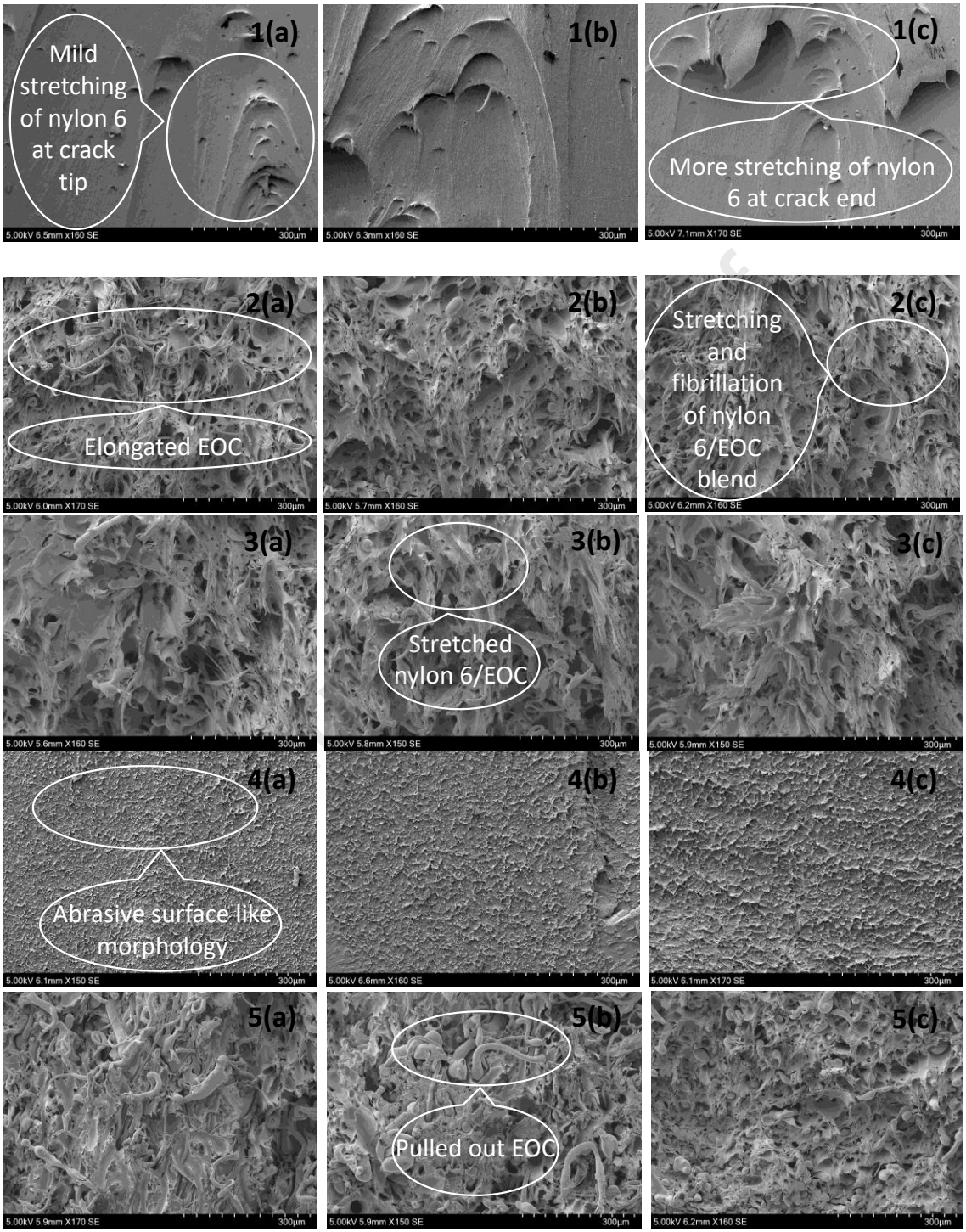

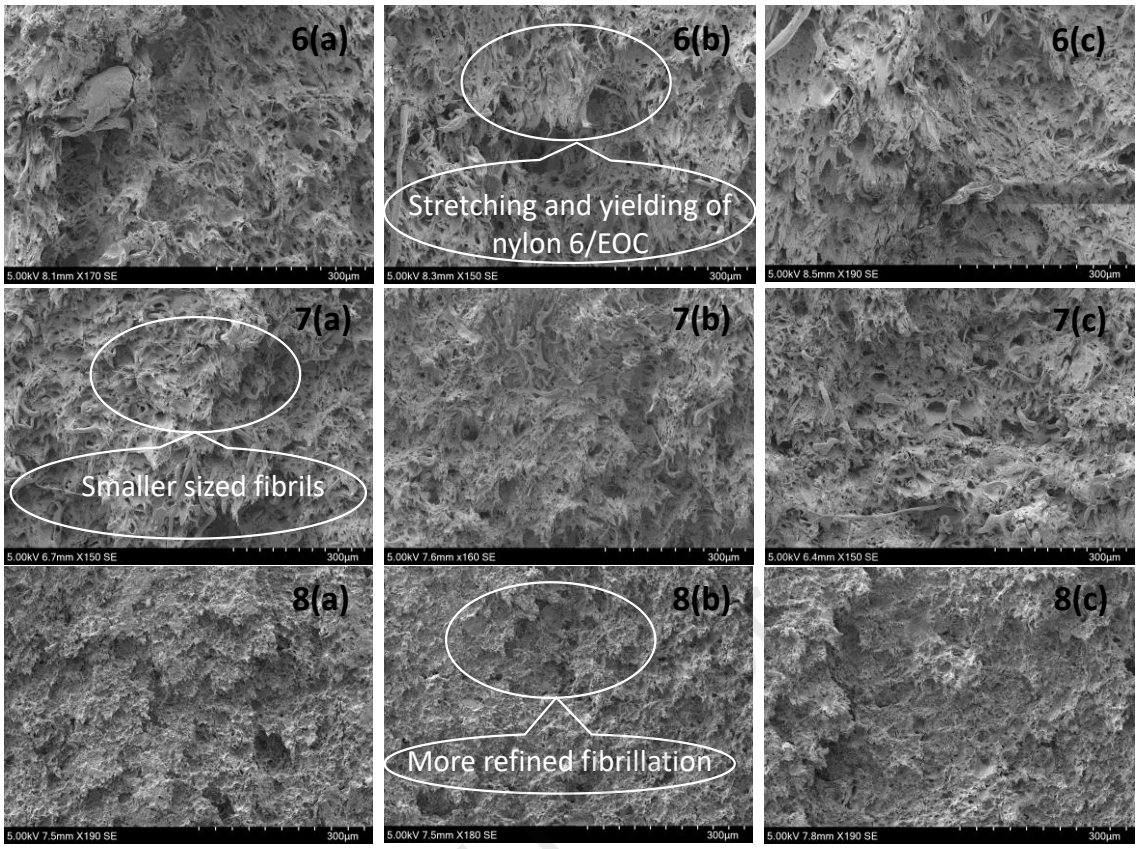

Figure 7 Low resolution SEM images of SENB tested samples at (a) crack tip, (b) crack middle and (c) crack end for (1) Nylon 6, (2) Nylon 6/EOC, (3) Nylon 6/EOC/EOC-g-MA, (4) Nylon 6/3% GnPs, (5) Nylon 6/EOC/3% GnPs, (6) Nylon 6/EOC/EOC-g-MA/3% GnPs (7) Nylon 6/EOC/EOC-g-MA/5% GnPs and (8) Nylon 6/EOC/EOC-g-MA/10% GnPs

4. Conclusions

Stiffness of the nylon 6 was increased by the addition of graphene nanoplatelets (GnPs) and increasing GnPs content also positively influenced the stiffness. It can be concluded that the stiffness of polymer nanocomposites is enhanced by the addition of stiff nanoparticles and their loading level. Tensile strength was also mildly increased by the addition of GnPs, however it can be postulated, based on the findings, that the tensile strength is mainly dependent on the strength of the interface and not much on the loading level of GnPs. The interfacial strength is observed to be dependent on the chemical nature of the nanoparticles and the presence or absence of functional groups. Increase in the

elongation at break of nylon 6 by the addition of high surface area GnPs could be a possible outcome of slippage of polymer chains facilitated by the GnPs. This caused an increase in the ductility and toughness of nylon 6. Impact strength of the blend-based nanocomposites was also positively influenced by the addition of GnPs which demonstrated the potential of simultaneous addition of stiff and elastomeric additives in enhancing the impact strength. Addition of Ethylene-octene copolymer (EOC) and maleated EOC (EOC-g-MA) to nylon 6 caused an increase in the elongation at break but adversely effected the stiffness and tensile strength. This was possibly due to the elastic nature of EOC while the addition of GnPs to nylon 6/EOC blends helped to regain the reduction in stiffness and tensile strength. Furthermore, the improvement in the fracture toughness indicated that compatibilized blend-based nanocomposites offered higher resistance to crack propagation. SEM scans showed that the fracture surface morphology of nanocomposites, tested under high and low strain rates, was very different which has likely influenced the mechanical properties. Also, addition of EOC-g-MA and different wt% of GnPs significantly altered the morphology from one case to the other as observed in the SEM images. This study showed that a balanced combination of tensile, impact and fracture toughness properties can be achieved by using a combination of stiff and elastomeric fillers under optimum loading levels and processing conditions.

Acknowledgements

The authors gratefully acknowledge the financial support of the project ICONIC — Improving the Crashworthiness of Composite Transportation Structures. ICONIC has received funding from the European Union's Horizon 2020 research and innovation programme under the Marie Skłodowska-Curie grant agreement No 721256. The content

in this paper reflects only the researchers' view and the Agency is not responsible for any use that may be made of the information it contains.

References

[1] I. Gonza´lez, J. I. Eguiaza´bal, and J. Naza´bal, "Nanocomposites based on a polyamide 6/ maleated styrene – butylene-co-ethylene – styrene blend : Effects of clay loading on morphology and mechanical properties," Eur. Polym. J., vol. 42, pp. 2905–2913, 2006, doi: 10.1016/j.eurpolymj.2006.07.014.

[2] F. C. Chiu and I. N. Huang, "Phase morphology and enhanced thermal/mechanical properties of polyamide 46/graphene oxide nanocomposites," Polym. Test., vol. 31, no. 7, pp. 953–962, 2012, doi: 10.1016/j.polymertesting.2012.06.014.

[3] A. Hassan, N. Othman, M. U. Wahit, L. J. Wei, A. R. Rahmat, and Z. A. Mohd Ishak, "Maleic anhydride polyethylene octene elastomer toughened polyamide 6/polypropylene nanocomposites: Mechanical and morphological properties," Macromol. Symp., vol. 239, pp. 182–191, 2006, doi: 10.1002/masy.200690095.

[4] N. Dayma and B. K. Satapathy, "Microstructural correlations to micromechanical properties of polyamide-6/low density polyethylene-grafted-maleic anhydride/nanoclay ternary nanocomposites," Mater. Des., vol. 33, no. 1, pp. 510–522, 2012, doi: 10.1016/j.matdes.2011.04.057.

[5] M. U. Wahit, A. Hassan, Z. A. M. Ishak, and T. Czigány, "Ethylene-octene copolymer (POE) toughened polyamide 6/polypropylene nanocomposites : Effect of POE maleation," Express Polym. Lett., vol. 3, no. 5, pp. 309–319, 2009, doi: 10.3144/expresspolymlett.2009.39.

[6] V. Tanrattanakul, N. Sungthong, and P. Raksa, "Rubber toughening of nylon 6 with epoxidized natural rubber," Polym. Test., vol. 27, no. 7, pp. 794–800, 2008, doi: 10.1016/j.polymertesting.2008.05.013.

[7] I. Gonza´lez, J. I. Eguiaza´bal, and J. Naza´bal, "Rubber-toughened polyamide 6/clay nanocomposites," Compos. Sci. Technol., vol. 66, no. 11–12, pp. 1833–1843, 2006, doi: 10.1016/j.compscitech.2005.10.008.

[8] W. S. Chow and Z. A. M. Ishak, "Polyamide blend-based nanocomposites : A review," Express Polym. Lett., vol. 9, no. 3, pp. 211–232, 2015, doi: 10.3144/expresspolymlett.2015.22.

[9] F. Chiu, S. Lai, Y. Chen, and T. Lee, "Investigation on the polyamide 6/organoclay nanocomposites with or without a maleated polyolefin elastomer as a toughener," Polymer (Guildf)., vol. 46, no. 25, pp. 11600–11609, 2005, doi: 10.1016/j.polymer.2005.09.077.

[10] I. Kelnar, J. Rotrekl, J. Kotek, L. Kaprálková, and J. Hromádková, "Effect of montmorillonite on structure and properties of nanocomposite with PA6/PS/elastomer matrix," Eur. Polym. J., vol. 45, no. 10, pp. 2760–2766, 2009, doi: 10.1016/j.eurpolymj.2009.06.024.

[11] H. Kim, A. A. Abdala, and C. W. Macosko, "Graphene/Polymer Nanocomposites," Macromolecules, vol. 43, pp. 6515–6530, 2010, doi: 10.1021/ma100572e.

[12] T. D. Thanh, L. Kaprálková, J. Hromádková, and I. Kelnar, "Effect of graphite nanoplatelets on the structure and properties of PA6-elastomer nanocomposites," Eur. Polym. J., vol. 50, no. 1, pp. 39–45, 2014, doi:

10.1016/j.eurpolymj.2013.10.022.

[13] F. Alirezaei Hoor, J. Morshedian, S. Ahmadi, M. Rakhshanfar, and A. Bahramzadeh, "Effect of Graphene Nanosheets on the Morphology, Crystallinity, and Thermal and Electrical Properties of Super Tough Polyamide 6 Using SEBS Compounds," J. Chem., vol. 2015, pp. 1–6, 2015, doi: 10.1155/2015/819580.

[14] I. Kelnar et al., "Effect of Graphene Oxide on Structure and Properties of Impact-Modified Polyamide 6," Polym. Plast. Technol. Eng., vol. 57, no. 9, pp. 827–835, 2018, doi: 10.1080/03602559.2017.1354223.

[15] O. Norhayani, H. Azman, R. A. Razak, and W. M. Uzir, "Effects Of POE and POE-G-MA on impact and tensile properties of polyamide nanocomposites," in Simposium Polimer Kebangsaan Ke-V, 2005, no. May 2014.

[16] S. Lim, A. Dasari, G. Wang, Z. Yu, Y. Mai, and Q. Yuan, "Impact fracture behaviour of nylon 6-based ternary nanocomposites," Compos. Part B, vol. 41, no. 1, pp. 67–75, 2010, doi: 10.1016/j.compositesb.2009.03.006.

[17] W. S. Chow, Z. A. M. Ishak, J. Karger-kocsis, A. A. Apostolov, and U. S. Ishiaku, "Compatibilizing effect of maleated polypropylene on the mechanical properties and morphology of injection molded polyamide 6/polypropylene/organoclay nanocomposites," Polymer, vol. 44, no. 24, pp. 7427–7440, 2003, doi: 10.1016/j.polymer.2003.09.006.

[18] X. Fu, C. Yao, and G. Yang, "Recent advances in graphene/polyamide 6 composites: A review," RSC Adv., vol. 5, no. 76, pp. 61688–61702, 2015, doi: 10.1039/c5ra09312k.

[19] D. Vroom, "Thermal and mechanical analysis of nylon 6 and nylon 6 , 6 blends,"

1997.

[20] C. Wan and B. Chen, “Reinforcement and interphase of polymer/graphene oxide nanocomposites,” J. Mater. Chem., vol. 22, no. 8, pp. 3637–3646, 2012, doi: 10.1039/c2jm15062j.

[21] R. J. Young et al., “The mechanics of reinforcement of polymers by graphene nanoplatelets,” Compos. Sci. Technol., vol. 154, pp. 110–116, 2018, doi: 10.1016/j.compscitech.2017.11.007.

[22] M. Karevan and K. Kalaitzidou, “Formation of a complex constrained region at the graphite nanoplatelets-polyamide 12 interface,” Polymer, vol. 54, no. 14, pp. 3691–3698, 2013, doi: 10.1016/j.polymer.2013.05.019.

[23] X. Zhu and J. A. Joyce, “Review of fracture toughness (G , K , J , CTOD , CTOA) testing and standardization,” Eng. Fract. Mech., vol. 85, no. May, pp. 1–46, 2012, doi: 10.1016/j.engfracmech.2012.02.001.

[24] A. S. Argon and R. E. Cohen, “Toughenability of polymers,” Polymer, vol. 44, no. 19, pp. 6013–6032, 2003, doi: 10.1016/S0032-3861(03)00546-9.

[25] B. Cotterell, J. Y. H. Chia, and K. Hbaieb, “Fracture mechanisms and fracture toughness in semicrystalline polymer nanocomposites,” Eng. Fract. Mech., vol. 74, no. 7, pp. 1054–1078, 2007, doi: 10.1016/j.engfracmech.2006.12.023.

Supplementary information

A schematic of tension and compression modes of the Izod impact test along with measured impact strength values are shown in Figure 1 (a and b). Neat nylon 6 exhibited the highest Izod impact strength of 58.1±5.3 kJ/m^2 and corresponding nanocomposites had an Izod impact strength of 33.8±2.1 kJ/m^2. This reduction can be attributed to the constraining of polymer chains and presence of stiff nanoparticles. Nylon 6/ Ethylene-octene copolymer (EOC) blend showed an Izod impact strength of 14.5±1.8 kJ/m^2 and nylon 6/EOC blend based nanocomposites had an impact strength of 10.8±0.5 kJ/m^2.

Addition of the compatibilizer, maleated EOC (EOC-g-MA), caused a slight increase in the Izod impact strength, as compared to uncompatibilized nylon 6/EOC blend, with an impact strength value of 21.1±1.8 kJ/m^2. This increase in the impact strength is likely due to the occurrence of some energy dissipation phenomena introduced by the GnPs. Higher contents of GnPs i.e. 5 wt%, 10 wt% and 15 wt% caused an increase in impact strength as compared to the compatibilized blend. However, their impact strength was still lower than that of neat nylon 6.

Izod specimens were tested in the compression mode to study the behaviour of developed nanocomposites under compression loading. When the material fractures under compressive loading, the atoms or molecules of the material slide past each other which creates interatomic/ intermolecular friction. This causes an increase in the impact strength of the material under compressive loading condition as compared to the impact strength under tensile loading (crack opening mode) where there is no internal friction. Since compressive loading conditions exist in case of crash events, so compressive impact strength obtained by this test could be useful in understanding the nanocomposite

behaviour under these conditions. Izod impact strength of nylon 6 and blend-based nanocomposites tested in the compression (notch closing) mode is shown in Figure 1 (b). Neat nylon 6 exhibited an Izod impact strength (compression) of 231.8±5.2 kJ/m^2. A higher Izod impact strength of 268.6±4.1 kJ/m^2 was observed for nylon 6/GnPs nanocomposites. Nylon 6/EOC blend showed lower Izod impact strength (compression) than that of neat nylon 6. Addition of 3 wt% GnPs to nylon 6/EOC blend caused a further reduction in the Izod impact strength.

Compatibilized nylon 6/EOC blend showed almost similar impact strength as that of the nylon 6/EOC blend. Nanocomposites with 3 wt% GnPs and compatibilized nylon 6/EOC blend exhibited an impact strength value of 165.9±3.9 kJ/m^2. Addition of higher wt% content of GnPs in compatibilized blend caused a mild increase in the impact strength.

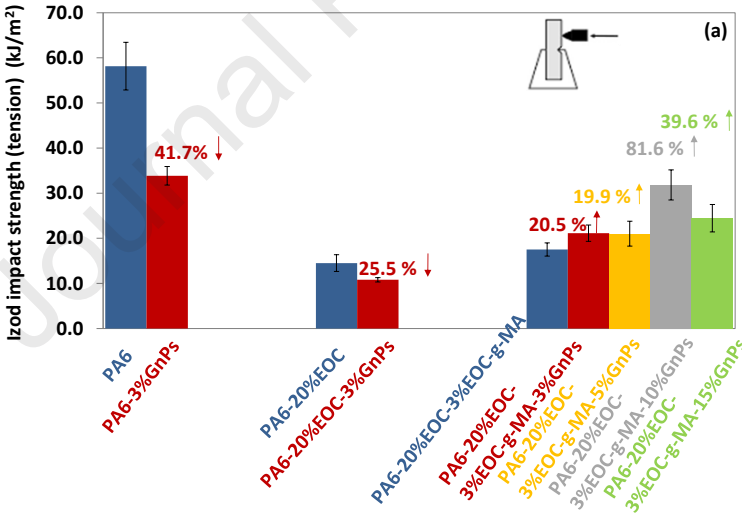

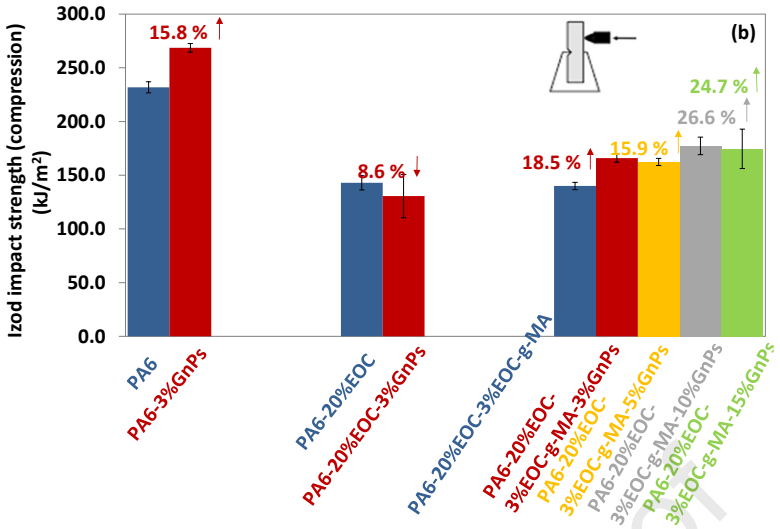

Figure 8 Izod impact strength (a) tension and (b) compression mode of nylon 6 and nylon 6 nanocomposites

Representative load-deformation curves of SENB specimens are shown in Figure 2.

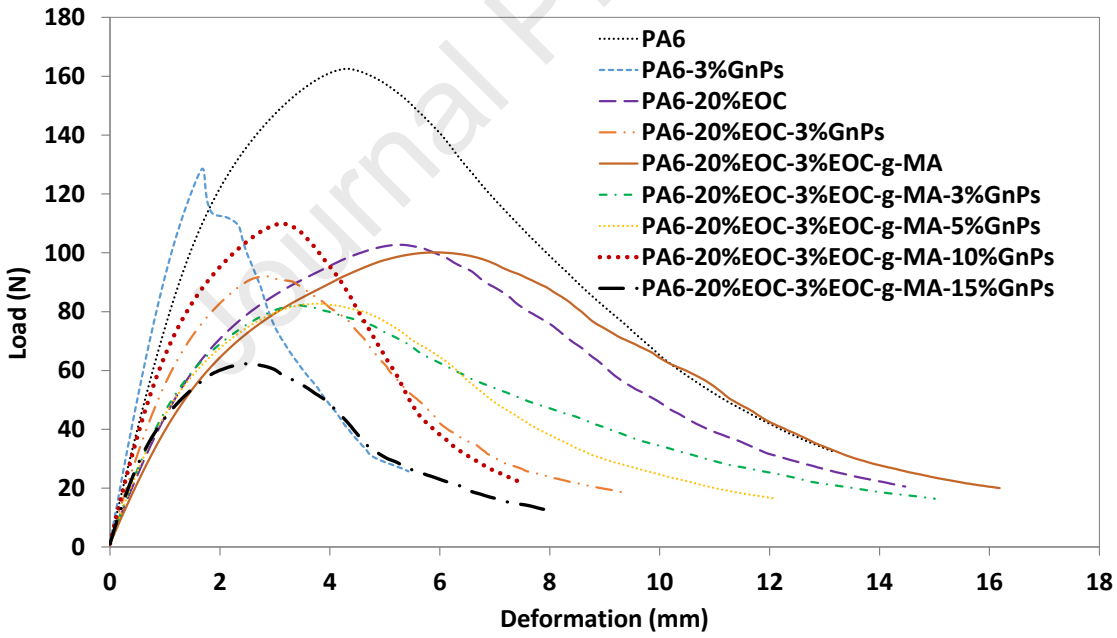

Figure 9 Representative load-deformation curves of SENB specimens for nylon 6 and nylon 6 nanocomposites

J-integral values corresponding to the different ligament lengths are shown below in Figure 3.

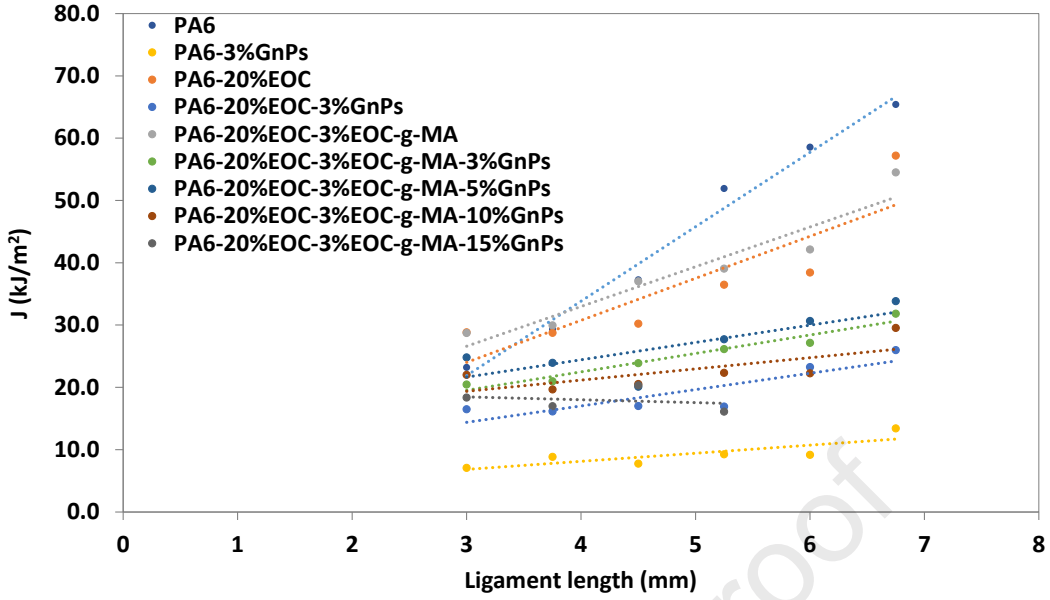

Figure 10 J-integral vs ligament length for nylon 6 and nylon 6/EOC/GnPs nanocomposites

Higher resolution SEM images of the fracture surface of SENB tested samples were also obtained to study the fracture phenomenon under quasi-static loading and compared with the fracture phenomenon in the case of high-speed impact loading. It was observed that a relatively smooth fracture surface was obtained for neat nylon 6 fractured under a quasi-static bending load as shown in Figure 4 (a). Small voids were observed on the fractured surface of nylon 6. The nylon 6/EOC blend underwent significant stretching and failure in the form of fibrils as seen in Figure 4 (b) possibly because of the slow drawing process. EOC particles stretched to elongated particles and ultimately broke. Compatibilized nylon 6/EOC blend also exhibited a similar morphology to that of uncompatibilized blend, however, with relatively larger fibrils. Entangled EOC particles were also observed on the fracture surface in Figure 4 (c).

Nylon 6/3 wt% GnPs nanocomposites showed a distinct fracture surface morphology to that of neat nylon 6 and nylon 6/EOC blends. Slight nylon 6 drawing took place as seen in the fracture surface morphology, however, due to stiff GnPs nanoparticles this

stretching was not extensive. A uniform fracture surface morphology was observed as shown in Figure 4 (d). A rough but plain fracture surface indicated a smooth crack propagation without much deflection which could be a cause of reduction of fracture toughness on nylon 6/GnPs nanocomposites as compared to neat nylon 6. Microvoids were observed in this nanocomposite sample which were not present in case of nylon 6/EOC blend. The presence of micro voids/porosity could be due to the immiscibility of nylon 6 with EOC or addition of GnPs to the blend. An increase in the fracture toughness of this blend-based nanocomposite was observed which could be due to the unique morphology obtained in this case. Compatibilized nylon 6/EOC blend-based nanocomposite exhibited stretching of the matrix and formation of fibrils as shown in Figure 4 (f). Compatibilized blend-based nanocomposite with 3 wt% GnPs exhibited a higher fracture toughness than uncompatibilized blend-based nanocomposite. In a similar way stretching of nylon 6 matrix and fibrillation was observed for 5 wt% and 10 wt% GnPs based nanocomposites. Nanocomposites based on 5 wt% GnPs showed smaller fibrils and a higher degree of fibrillation possibly due to a higher wt% of GnPs. A further refined fibrillation was observed in the case of 10 wt% GnPs based nanocomposites. Microvoids or pores were observed in the case of both 5 wt% and 10 wt% nanocomposites but 10 wt% nanocomposites showed higher degree of porosity. A progressive increase in the fracture toughness of the compatibilized nylon 6/EOC blend was observed by adding higher wt% of GnPs. It was observed that the fracture toughness of nylon 6/EOC blend based nanocomposite with 15 wt% GnPs surpassed that of the neat nylon 6. It can be postulated that the morphology attained by the simultaneous addition of EOC and GnPs facilitated more energy dissipation. Crack deflections or other energy dissipation phenomena occurring due to the addition of GnPs have likely increased because of

increasing content of GnPs. Higher resolution images showed the presence of microvoids and porous microstructure which was not clearly observed in low-resolution images.

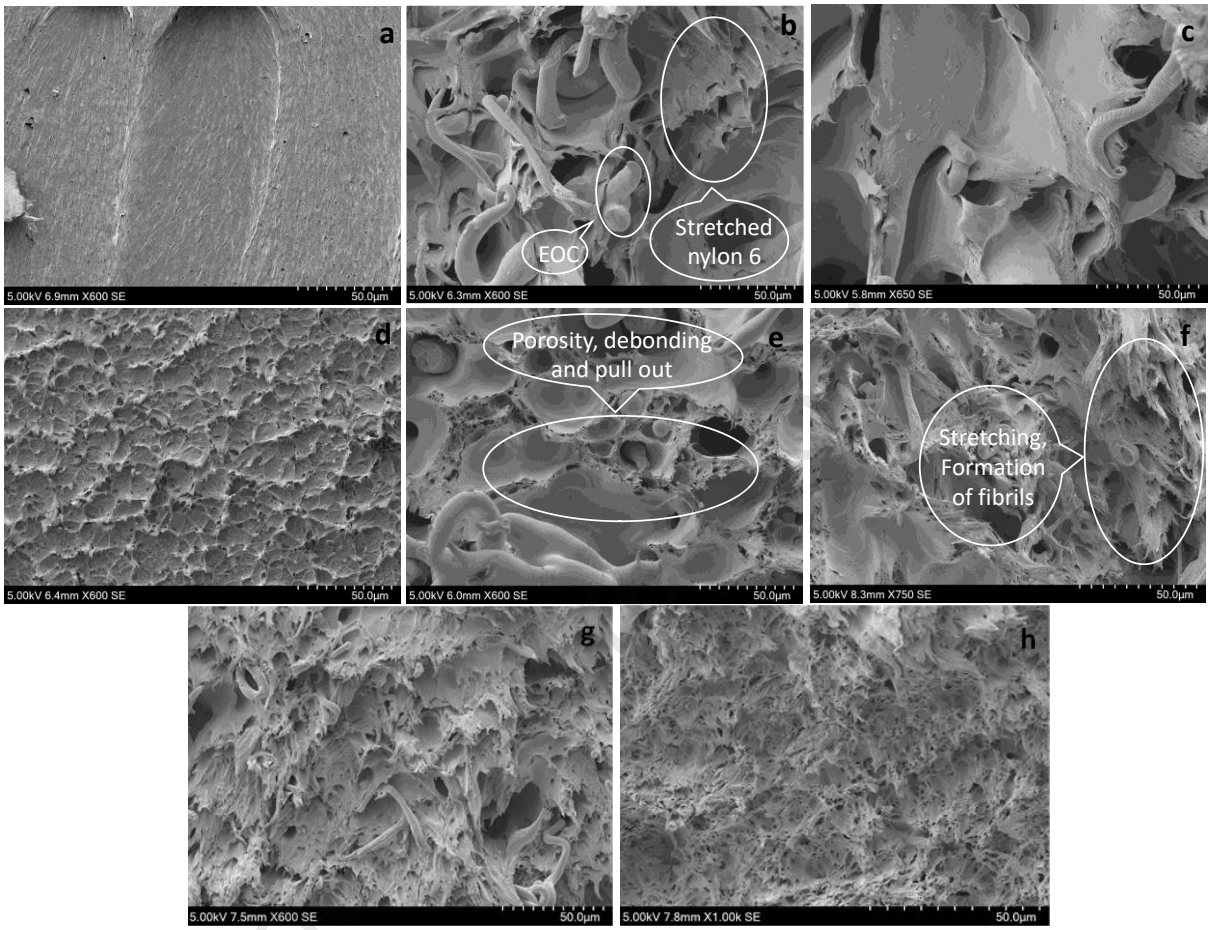

Figure 11 SEM images of SENB tested specimens (a) Nylon 6, (b) nylon 6/EOC, (c) nylon 6/EOC/EOC-g-MA (d) nylon 6/3 wt% GnPs, (e) nylon 6/EOC/3 wt% GnPs, (f) nylon 6/EOC/EOC-g-MA/3 wt% GnPs(g) nylon 6/EOC/EOC-g-MA/5 wt% GnPs(h) nylon 6/EOC/EOC-g-MA/10 wt% GnPs.

Table 1 DSC results for nylon 6, nylon 6/EOC and nylon 6/EOC/GnPs nanocomposites

Sample ID	2nd Heating			Cooling
	Melting Temp T_m (^oC)	Enthalpy of fusion ΔH (J/g)	% Crytallinity X_c (%)	Crystallization Temp T_c (^oC)
PA6	220.1	70.5	37.5	189.0
PA6-20%EOC	220.8	57.5	38.2	188.8
PA6-20%EOC-3%EOC-g-MA	220.7	46.8	32.3	188.7
PA6-3%GnPs	220.2	64.1	35.1	192.8
PA6-20%EOC-3%GnPs	220.2	58.8	40.6	191.9
PA6-20%EOC-3%EOC-g-MA-3%GnPs	219.9	53.9	38.7	192.5
PA6-20%EOC-3%EOC-g-MA-5%GnPs	219.9	49.8	36.8	192.5
PA6-20%EOC-3%EOC-g-MA-15%GnPs	219.2	42.6	36.5	193.3

Table 2 Tensile test results of nylon 6 and nylon 6 nanocomposites

Materials	Young's modulus (GPa)	Tensile strength (MPa)	Strain at break (%)	Toughness (J/m^3)
PA6	2.8±0.2	87.0±0.5	11.8±0.6	806.9±34.8
PA6+20%EOC	1.8±0.1	50.3±0.5	14.8±0.4	678.5±25.0
PA6+20%EOC+ 3%EOC-g-MA	1.5±0.1	40.2±0.2	54.6±1.8	2160.7±72.8
PA6+ 3%GnPs	3.3±0.1	77.4±0.4	15.0±0.5	979.6±31.9
PA6+20%EOC+ 3%GnPs	1.9±0.0	45.8±0.3	22.4±0.5	977.6±27.8
PA6+20%EOC+ 3%EOC-g-MA+3%GnPs	1.6±0.0	42.2±0.7	36.8±1.0	1487.3±39.2
PA6+20%EOC+ 3%EOC-g-MA+5%GnPs	1.8±0.0	42.6±0.4	34.6±1.1	1461.8±47.6
PA6+20%EOC+ 3%EOC-g-MA+10%GnPs	2.0±0.0	43.2±0.4	29.2±1.0	1264.2±54.5
PA6+20%EOC+ 3%EOC-g-MA+15%GnPs	2.2±0.1	44.7±0.8	19.4±0.4	837.0±23.7

Highlights

- Adding stiff nanoparticles and thermoplastic elastomer to nylon 6 can help achieve a balance of mechanical properties.
- Mechanical properties are enhanced through optimal nanoparticle loading and controlled processing conditions.
- The morphology of the nanocomposite strongly influences its mechanical properties.
- Ethylene-octene copolymer, along with malleated ethylene-octene copolymer, serves as a strong toughening agent for nylon 6.

Declaration of interests

☒ The authors declare that they have no known competing financial interests or personal relationships that could have appeared to influence the work reported in this paper.

☐The authors declare the following financial interests/personal relationships which may be considered as potential competing interests: